

O. Gökgöl  
Messerschmitt-Bölkow-Blohm  
Unternehmensbereich Hamburg

### Abstract

This study discusses the crack-free and cracked life of the fuselage including the fin box of the Airbus A 300 B and the problems involved.

Structural design details and dimensioning aims with reference to the service life are presented. The calculation methods for the determination of stress distribution within the structure and for assessment of the crack-free and cracked life and residual strength are described. The residual strength and fatigue tests on minor and major components aimed at detail optimization and full scale fatigue tests for the purpose of demonstration an adequate service life and the damage tolerance properties under simulated operational conditions are discussed. The test results are evaluated and compared with the design aims.

With damages occurring before the specified life aim is reached, the causes and repercussions on the damage tolerance behaviour of the structure are studied. The modifications carried out and the life improvements thus achieved are presented.

Inspection programs were established to guarantee a satisfactory damage tolerance behaviour. The kind and frequency of inspections is determined according to a directive whose details are briefly summarized in this study.

### I. Introduction

The A 300 B aircraft is a cooperative effort by France, Germany, Great Britain, USA, Spain and the Netherlands. The work sharing regarding manufacture of the structure is as follows:

MBB: Fuselage sections from the tail cone to section 16, upper shell of section 15, and the vertical tail

VFW-Fokker: Fuselage sections 13 and 14

AS: Flight compartment, fuselage sections 12, 15 (lower shell), wing centre box and pylons

CASA: Horizontal tail and passenger compartment door No. 1

Fokker-VFW: Movable components on the wing, flap track fairings

British Aerospace (HSA): Cantilever wing, slats

General Electric: Engines

Messier: Landing gears

The design of the A 300 B was based on many years' experience gained on aircraft like the Trident (HSA) and the Caravelle (AS). Furthermore, by means of extensive studies and tests, bases were created to ensure reliability of the structure and to achieve an optimum design regarding weight and

cost.

The structural layout, with respect to fatigue, was made as per specification FAR-Part 25 and the specifications established by the Franco-German certification authorities.

The Airbus A 300 B was intended for short- and medium-range service. The layout aims, with respect to fatigue, are as follows:

- . 24000 flights crack free
- . up to 32000 flights with minor repairs
- . 48000 flights "economic repair life"

In order to meet these life requirements and to ensure a high level of reliability throughout the service period, the following aspects had to be considered in particular:

#### Design Stage

The individual components of the structure were dimensioned in such a way that optimum strength/weight relation was obtained. A computer program (ASKA), operating by the Finite Elements Method, served as a basis for this. The calculated stresses were checked, by extensive stress measurements on the static test rig, for all relevant load cases.

#### Structure

The load carrying structure of the fuselage and the fin box consists of high strength Al alloys, a few steel or titanium fittings excepted. The leading edge of the fin box, and the fairings between rudder and vertical stabilizer as well as between elevator and horizontal stabilizer, and the horizontal tail tips are of GRP.

With the design of the structure, optimum quality was aimed at. The requirements regarding damage tolerance were met in so far as in the case of a fatigue damage, the adjacent components took over the loads of the failed element. In places where this was not possible, slow growth of the fatigue cracks was provided, either by a low stress level or by a reasonable arrangement of material accumulations, so that such damages can be detected and repaired by scheduled inspections.

#### Manufacture

To a larger extent, integral construction was used, with most modern NC machining processes being applied. At least 3 mm were removed on the surface of blanks, in order to exclude metal enclosures, bulges and surface cracks from the rolling process.

The surfaces of the machined components were mostly shot-peened intensively, and the fastening elements of steel and titanium were installed with oversize, if locally no particular fits for design reasons were specified.

For skin/stringer connections throughout the fuselage, except in the lower fuselage area where

stringers are riveted, the hot-bonding method was applied.

Extensive corrosion protection for semi-finished materials (sheets, frame and stringer sections, connecting plates, doublers etc.) was cared for prior to assembly already. The corrosion protection applied (Airbus code No. 3 + 281 NT 00//A007.10003) was tested in extensive long-term tests under extreme weather conditions.

The manufacture of equipment involved great expenditure, for exact fitting was aimed at; as a result, rework on assembly and thus damage to the surface protection do not occur.

## II. Damage Tolerance

The requirements under § 25.571, Part 25 of the Federal Aviation Regulations specify that strength, design, and manufacture of the structure must be of such a constitution that a catastrophic failure of the aircraft, due to fatigue, corrosion or damages caused by accidents, is not possible during the envisaged service life.

Life and crack growth studies proved, for the load-carrying structure of the A 300 B, that in the case of damages due to fatigue, corrosion, or external damage, within the envisaged service life of the aircraft, the remaining cross sections will hold, without failure and/or without inadmissible deformations, until the damages are detected.

A residual strength analysis was carried out on the principal structural elements of the pressurized cabin to show that the remaining structure is able to withstand loads corresponding to the following conditions:

- the normal operating pressure combined with the expected external aerodynamic pressures applied simultaneously with the flight loading conditions if they have a significant effect.
- the expected external aerodynamic pressures in lg-flight combined with a cabin differential pressure equal to 1,1 times the normal operating pressure without any other load.

Principal structural elements, which contribute significantly to carrying flight, ground and pressurization loads, and whose failure could result in catastrophic failure of the airplane are:

### Fuselage:

- Circumferential frames and adjacent skin
- Door frames
- Pilot window posts
- Pressure bulkhead
- Skin and any single frame or stiffener element around a cutout
- Skin or skin splices, or both, under circumferential loads
- Skin or skin splices or both, under fore-and-aft loads
- Skin around a cutout

- Skin and stiffener combinations under fore-and-aft loads
- Window frames

### Fin Box:

- Primary Fittings, lugs, bolts
- Principal splices
- Skin or reinforcement around cutouts or discontinuities
- Skin-stringer combinations
- Spar caps
- Spar webs

According to appendix H of the new FAA regulations under § 25.571 it is allowed to apply the damage tolerance (fail-safe) evaluation approach to both the single load path and multiple load path structure. It is possible, by sufficient analysis and testing, to establish that a single load path structure has sufficiently slow crack growth properties so that, if a crack were to develop, it would be discovered during a properly designed inspection program.

According to this regulation, the stress level was kept low in all longitudinal and circumferential splices of the pressurized cabin and pressure bulkhead paneling, as well as in all lug connections, in order to keep the growth rates of possible cracks low. This safety measure for the skin splices was considered necessary for the possibility that fatigue cracks should start from several adjoining rivets simultaneously and form one common crack.

The intervals between the scheduled inspections of the skin splices were ascertained by the microfractographical evaluation of fatigue cracks from the full-scale fatigue tests, taking into account a safety factor of 2.0.

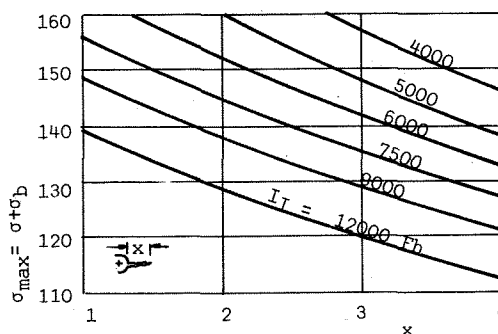


Figure 1. Inspection (NDT) Intervals for the Longitudinal Splice of the Pressurized Cabin

For skin and stiffener combinations, the damage tolerance evaluation (calculation and test) was carried out for the following cases:

- Two-bay longitudinal crack in skin with the centre frame intact

- Two-bay longitudinal crack in skin with the centre frame failed
- Two-bay circumferential crack in skin with the centre longeron failed
- Skin crack between two intact longerons or frames.

Due to crack growth and residual strength tests on fuselage part-shells<sup>(1)</sup>, which were carried out during the design stage of the A 300 B already, the stiffener cross sections and the frame and stringer pitches were arranged in such a way that major skin cracks are stopped by the adjacent stiffeners.

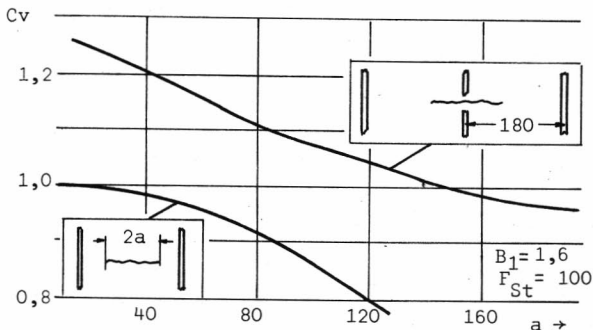


Figure 2. Tip Stress Ratios for Circumferential Cracks in the Fuselage Skin

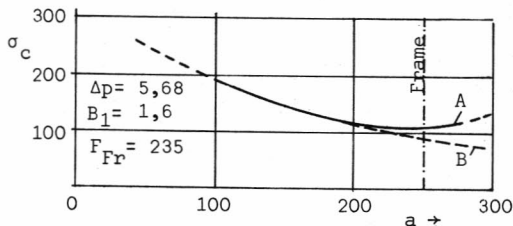


Figure 3. Residual Strength of the Fuselage Skin for a Longitudinal Crack between two Intact Frames

### III. Configuration Candidates

With the arrangement of the shell structure, the FAA requirements concerning life and fail-safe properties were authoritative.

In order to ensure slow crack growth and sufficient residual strength, the material 2024 (Alclad) (3.1364.4) was chosen for the paneling of the fuselage. Skin thicknesses are 1.6 - 2.0 mm in the pressurized cabin, 1.4 - 1.0 mm in the pressure bulkhead. Optimum use of the material of the paneling was reached by:

- arranging the longitudinal splices as lap joints with two rivet rows; with this, the longitudinal splices exposed to higher loads (radial loading = 1600 N/cm) were provided with a bonding doubler of 0.6 mm thickness.
- tapering the skin panels between frames and stringers in the undisturbed area by chemical milling

The following illustration shows a section through the joint in the area of load transmission from the paneling end to the fuselage attach fitting.

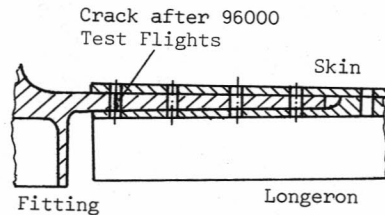


Figure 4. Riveting of the Fuselage Fitting at the Fin Box (see Photo in Fig. 24-KS 20)

One of the typical places in the pressurized cabin, which are most frequently affected by fatigue damages, is the skin connection at the base of the frame. On the A 300 B, the frame/skin connection is effected by clips manufactured from 1.2 mm sheet metal of 2024 T4. The riveting to the fuselage skin was optimized, during the design phase already, to the effect that in the full-scale tests of the pressurized cabin sections no skin cracks were detected at the clip end rivets.

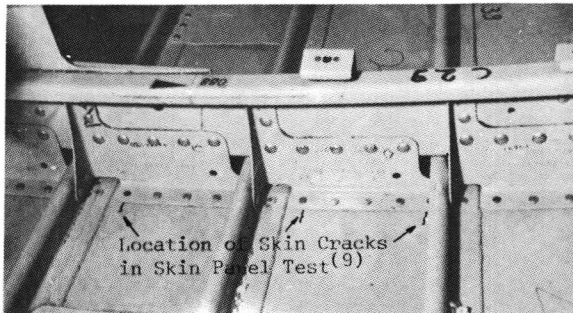


Figure 5. Frame Clips

The stringer couplings were manufactured from 2024-T351. They are intensively shot-peened and connected to the paneling by Titanium rivets.

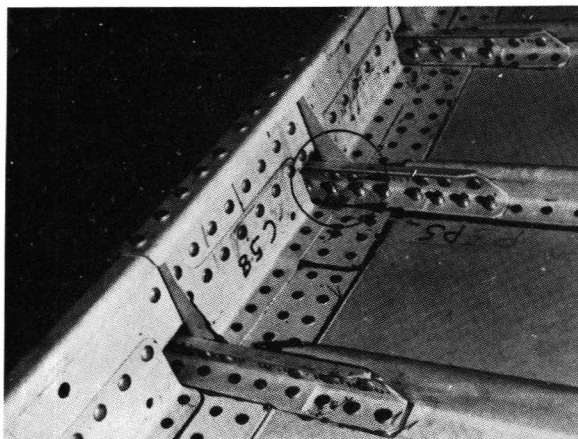


Figure 6. Stringer Couplings

Further typical structural details, like the fail-safe passenger compartment door frame, the integral machined floor cross beams (2024-T351) are illustrated in figure 7.

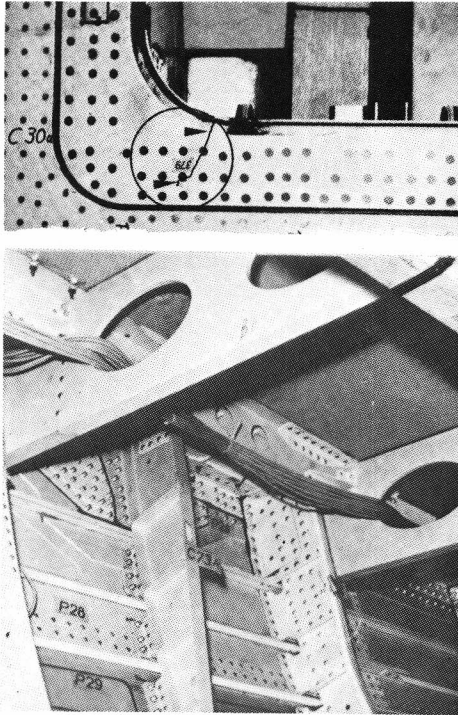


Figure 7. Fail-safe Frame on the Passenger Door and Integrally Machined Floor Beams

With these integral components, shot-peening was confined to radii, adjoining surfaces, and those areas where increased operational stresses and possible assembly stresses were to be expected. The remaining surfaces were treated with less intensity. On chemically milled skin panels, these areas were shotpeened (with less intensity) only, if the depth of material to be removed exceeded 0.4 mm.

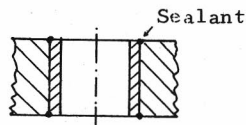


Figure 8. LM-Lugs with Interference Fit Bushes

All light metal lug connections were provided with a cadmium-plated oversize bushing of stainless steel, which were sealed (PR 1421) on the front. The bushing oversize entails a life increase by factor 2 and above for the lug.

#### IV. Calculation of Crack-Free Life, Cracked Life and Residual Strength

For all components of the fuselage and the fin box which are considered critical with respect to fatigue, the life was calculated already in the design phase. These studies were based on stresses

which had been ascertained by calculations or - as far as existing - by measurements.

The stresses in the structure for the different load cases were ascertained by two separate calculations for the pressurized cabin/MBB-UH share (8400 unknown quantities, 20000 cross sections) and for the aft fuselage with the vertical tail (4800 unknown quantities, 11000 cross sections). For this purpose, a computer program (ASKA) was used, which operates by the Finite Elements Method.

Ascertainment of the load spectrum was based on the following static load cases:

- $n_z = 1$  - loads
- internal pressure
- taxiing on ground, landing impact
- vertical and horizontal gusts
- lateral and longitudinal manoeuvres

Flight by flight stress spectra for the envisaged service life were established, for calculation and test. Part collectives of gust loads for the individual flight phases of individual flights were ascertained by EDP computation. For each component examined, the stress history throughout one flight was drawn, and the stress amplitudes as well as the basic stress are read off by the peak-to-peak method.

#### Calculation of Crack-Free Life

The crack-free life was ascertained as per the linear damage accumulation method by Palmgren - Miner. For the majority of the components examined, Wöhler-curves from life tests could be utilized, under consideration of possible negative deviations of the sample from the population.

As result of the fatigue calculations for the individual components (for 47040 service flights and 960 checkout test flights) the failure probability with reference to the first crack to be inspected was determined.

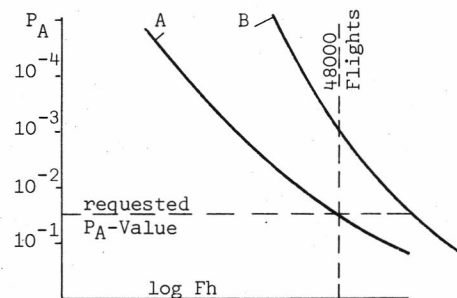


Figure 9. Calculated  $P_A$ -Values for Component A and B

For the correct execution of such a reliability analysis it is necessary that both the deviations of the load collective and of the utilized Wöhler-curves are known. In case of single flights which are described by a variety of load collectives it takes more trouble however to determine the overall deviation of the end product even if the probability of the partial collectives to occur are known.

A simplified method of approach to this problem lies in the fact that for setting up a single flight partial collectives with a 50% probability of occurrence are used. The occurrence probability of the single flight collective is then 50% also.

The trace of the reliability curve above the service life curve can be regarded to be correct only in the  $P_A = 50\%$  level. For smaller  $P_A$ -values errors in the life estimation must be taken into account.

The following figure illustrates this schematically:

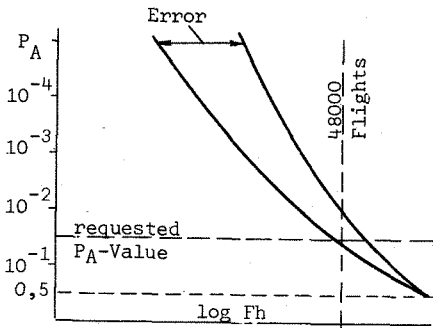


Figure 10. Accuracy of Life Estimation as Function of Requested  $P_A$ -Level

All tested fuselage and fin box components had been designed to the fail-safe principle and for most of them failure probabilities between  $10^{-2}$  and  $10^{-1}$  were specified depending on the cost of repairs. Thus the collective conditioned errors in the calculated life estimation were insignificant. The above illustration shows however that in the case of specified  $P_A$ -values of  $10^{-4}$  and less (safe-life requirements) uncertainties in the load collective with reference to the occurrence probability can cause an insecure life estimation.

#### Calculation of Cracked Life and Residual Strength

Calculation processes, introduced by Forman, operating to the stress intensity concept were used to determine the calculated life proof of the cracked structure.

Accordingly the crack propagation rate in a skin area is dependant on the stress intensity amplitude

$$\Delta K = K_{max} - K_{min}$$

and the fracture toughness of the material  $K_c$ .

The stress intensity amounts to:

$$K = \sigma \cdot \sqrt{\pi \cdot a} \cdot C \cdot C_1 \cdot C_v$$

The residual strength  $\sigma_c$  is dependant on the maximum stress intensity and on the fracture toughness.

$$\sigma_c = K_c / (\sqrt{\pi \cdot a} \cdot C \cdot C_1 \cdot C_v)$$

Intact stiffeners in the neighbourhood or above the skin cracks reduce the stress intensity and thereby the crack propagation rate and increase the residual strength of the cracked structure. This is effected by transferring the forces from the cracked

skin to the stiffeners.

An EDP-program was established which determines the stress tip ratio (2)

$$C_v = (K_{(stiffened)} / K_{(unstiffened)})$$

and the stringer load factor

$$L_s = (P_{str(max)} / P_{str(a=0)})$$

depending on the stiffness of the fasteners (stringer riveting).

Rivet deformation has already been considered as to Swift<sup>(3)</sup>

$$\delta = \frac{N}{E_N \cdot d} \left\{ 5.0 + 0.8 \left( \frac{d}{B_1} \frac{E_N}{E_H} + \frac{d}{B_2} \frac{E_N}{E_{str}} \right) \right\}$$

In figure 3 curves A and B show the critical stress for a stiffened and an unstiffened skin. Considering the fact that in both cases equal stress intensity is decisive for crack propagation, the difference between A and B is:

$$C_v = \sigma_{c(B)} / \sigma_{c(A)}$$

In the scope of calculated crack propagation and residual strength tests for the Airbus skin cracks lying centrally under a broken stringer (frame) were tested also. Figure 2 shows that in such a case  $C_v > 1.0$  applies, i.e. the stress intensity increases beyond values of the unstiffened field. The cracked life of the skin area is then negatively influenced.

The influence of additional shear in connection with tensile stresses acting transversely to the crack was also taken into consideration. Analogue to the crack opening type I

$$K_1 = \sigma \sqrt{\pi \cdot a}$$

for the plain shear stress (crack opening type II) the stress intensity is:

$$K_2 = \tau \sqrt{\pi \cdot a}$$

and for the case of a combined load application the critical stress intensity is:

$$(K_{1c})^2 = K_1^2 + 1,78 K_2^2$$

Up to the present, little experience has been made with regard to the relation between the bi-axial stress condition and the intensity of stress at the crack tip. Evaluations of crack propagation<sup>(4)</sup> performed at MBB-UH showed that negligence of the 2<sup>nd</sup> stress in crack direction results in considerable errors in the calculatory simulation of crack propagation.

Calculation of the cracked life is performed to the equation:

$$(da/dn) = \{M \cdot (\Delta K)^n\} / \{(1-R)K_c - \Delta K\}$$

For the determination of cracked life an EDP-<sup>(5)</sup> program was established into which the stiffener factors as a function of the crack length can be fed. This program also calculates the residual

strength of the structure by assuming that  $a = a_c$  if  $K_{max}$  reaches the value for  $K_c$ . The crack propagation rate  $da/dn$  then becomes infinite.

Figure 11 shows the "formalized" crack propagation data for the skin material.

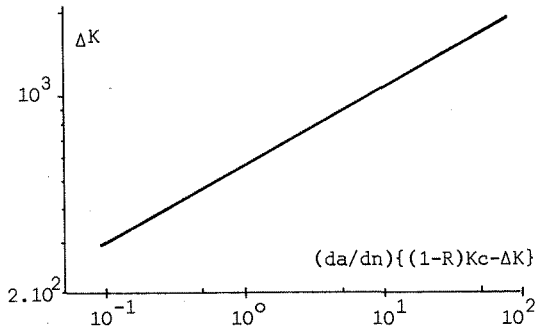


Figure 11. Formanized Crack Propagation Data for 2024-T3 ( $K_c = 3338$ )

In the case of multi-stage load applications the positive spectrum peak loads cause a retardation of crack propagation. If this effect is neglected in the calculations the above formulae lead to results which are on the safe side.

Another calculation program was established<sup>(6)</sup> for consideration of retardation due to peak loads in the calculation of crack propagation under multi stage load application. Stiffener factors and other factors influencing the stress intensity, can be fed into this particular program as well. This extended program was however used for reasons of cost only, if the influence of the load peaks on the cracked life had to be considered by all means.

Determination of Fatigue Ratings for the Establishment of an Inspection Program

First of all an inspection program was established for fuselage sections tested in full scale test and later on for the entire fleet.

For this purpose Structural Significant Items (SSI) within the structure were selected for which then the kind and frequency of inspections must be laid down as per the following aspects.

For the single SSI's first of all the fatigue rating was determined as function of their cracked life (crack propagation between an inspectable initial crack and that crack length at which crack propagation becomes unstable) and their location and at the same time it was defined whether the inspection must be carried out either externally (with direct access to SSI) or internally (no direct access to SSI).

The overall rating, the designation of which is shown in the following flow diagram is decisive for the ultimate definition of kind and frequency of inspections.

First of all the data from the life calculations were used to determine the overall ratings for the inspections of the full scale fatigue tests. With the life and crack propagation data obtained in the fatigue tests the inspection program for the A 300 fleet was laid down.

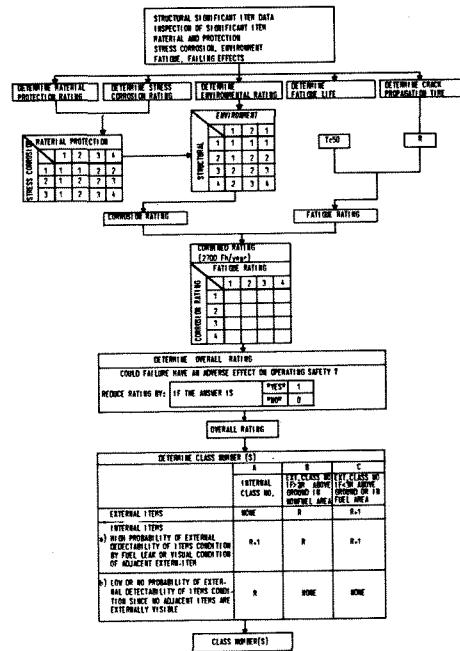


Figure 12. Flow Diagram to Determine the Inspection Ratings

V. Fatigue Tests

Airbus life and residual strength tests as well as fail-safe tests are subdivided into two groups:

- Testing of detail parts and of major assemblies for the optimization of design and for obtaining dimensioning stresses (partial tests)
- Full scale fatigue tests

V.1 Partial Tests

This group includes the following tests:

Report	Test (crack growth, residual strength)
TIV-001	Skin panel (3050 x 3268 mm) including frames, longerons and longitudinal
Ev-020	splices under internal pressure and longitudinal loads
Ev-050	Skin panel (3048 x 3268 mm) incl. windows, frames, stringers, longitudinal splices under internal pressure, longitudinal and torque loads
Ev-047	Pressurized bulkhead with complete fuselage section between frame no 78 and 81 under cabin pressure
Ev-048	Horizontal stabilizer actuator support under tailplane load spectrum (fail-safe verification due to removing of attachment bolts)
1.13.18	Lower rudder on vertical stabilizer (fail-safe verification)
Ev-049	Fuselage mounted fitting of rear horizontal stabilizer (fail-safe verification)
Ev-036	Vertical stabilizer fuselage connection (center spar vertical stabilizer mounted)

<u>Report</u>	<u>Test (crack growth, residual strength)</u>
	under vertical stabilizer load spectrum
Ev-037	Vertical stabilizer panel joint under vert. stabilizer load spectrum
Ev-039	Lateral force connection of vertical stabilizer rear spar under vertical stabilizer load spectrum

In addition to the component tests listed above, detail tests of minor components were carried out. As example the detail tests as part of the pressure bulkhead test under report no. Ev-047 shall be mentioned.

<u>Report</u>	<u>Detail Test (Fatigue)</u>
Ev-033	Stringer joint at frame 80 with pressure bulkhead
Ev-032	Ring bracket (connection pressure bulkhead-Fuselage)
Ev-029	Plate joint and meridian-stiffener from the pressure bulkhead
Ev-031	Pressure bulkhead joint at center spar

## V.2 Full Scale Fatigue Tests(8)

Four separate fuselage sections were subjected to full scale fatigue tests. Former experience from the fatigue testing justifies and confirms the advantages of multisection testing which are:

- fewer compromises in load spectrum
- tests on the four specimens running independently of each other
- faster execution of tests and therefore earlier identification of weak points and hence earlier incorporation of improvements required to eliminate them
- test facilities are less complex and cheaper
- earlier beginning of multisection testing compared with complete aircraft testing

The following sections were tested:

- A) Nose fuselage section
- B) Wing and centre fuselage section
- C) Aft fuselage section with fin box
- D) Tail plane section

In addition separate fatigue tests on nose and main landing gear were carried out. These tests and the tests under D) above are not included in this study.

10000 simulated flights on the full scale specimens (as required by the Airworthiness Authorities) had already been accomplished before the first flight of the Airbus A 300.

### Test Loading Procedure

Simulated flight and ground loads were applied to the structure through dual-action hydraulic jacks, transmitting both compression and tension loads.

Payload and inertia loads were applied to the passenger and cargo floor beams in the fuselage simulating the real distribution of a typical flight, the jack-rods passing through apertures

in the fuselage bottom skin, or top skin in the wing centre box and main U/C bay only.

The whole test was controlled by electronic computers. The required jack loads were punched on to a tape which was cycled through the computer. The actual jack loads were measured by load cells in the attachment to the cross-beam system and continuously compared with the required values and the test stopped if a significant difference occurred.

A large number of strain gauges was fitted to the structure whose readings were continuously checked and compared with the initial output at the beginning of the tests.

The pressurization load was applied by compressed air as in the real flight case. For safety reasons and in order to save time and energy the majority of the available fuselage volume was filled with blocks of expanded polystyrene foam so that the compressed air-volume was reduced by about 70 to 80%.

When dividing a complete fuselage into 3 smaller test specimens, it was necessary to extend the specimens beyond the area actually being tested in order to provide sufficient structure to distribute the applied test loads correctly over the cross-section of the fuselage. The correct distribution of loads in the fuselage is obtained only at some distance from the bulkhead. Since this phenomenon occurred on each test specimen, it follows that some overlap between the specimens was necessary so that every part of the structure was correctly loaded.

The correct distribution of stresses has been checked by means of strain gauge measurements on each test specimen and compared with measurements on the full-scale static test specimen which was a "one piece" specimen. The results showed a good correlation and justified the chosen overlap.

### A) Nose Fuselage Test

The nose fuselage specimen was tested in the VFW-Eokker factory in Lemwerder (near Bremen). As can be seen from fig. 13 the nose fuselage was cantilevered forward from a pressure bulkhead. All the applied ground and flight loads were reacted at the bulkhead.

The test specimen comprised:

- the primary structure of fuselage sections 11, 12, 13 and 14 including doors and windows
- the cockpit front windshields, the left hand lateral windshields and right hand rear windshield
- the passenger floor between frames 34 and 38 and floor straps between outer seat-rails and fuselage shell throughout section 14/13 and partly in section 12
- the cargo hold floor between frames 33 and 38

The fatigue test covered the justification for sections 11, 12, 13 and section 14 up to frame 33.

Section 14 from frame 33 to 39 was considered as a transition structure for correct loading distribution.



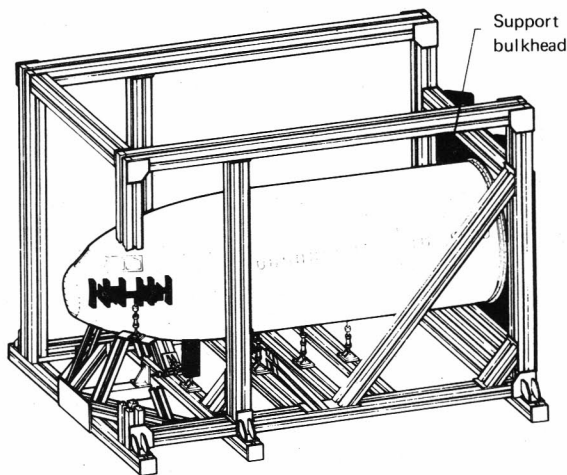


Figure 13. Fatigue Testing of the Front Fuselage

#### B) Centre Fuselage and Wing Test

The wing and centre fuselage section was tested in the IABG establishment in Ottobrunn (near Munich). Heavy bulkheads were fitted to the forward and aft end of the fuselage. As shown in Fig. 14 the test-specimen was suspended iso statically by means of hinged rods fixed to the bulkheads, all the applied ground and flight loads being reacted at these points.

The test specimen comprised:

- the primary structure of fuselage sections 14 to 17 including doors and windows
- the passenger floor between frames 30 and 34 (section 14), 58 to 62 and floor straps between outer seat rails and fuselage shell throughout section 14
- the cargo hold floor between frames 30 and 33 and frames 57 and 60
- the primary structure of the centre wing box
- the primary structure of the right and left hand wings
- the primary structure of the left hand engine pylon

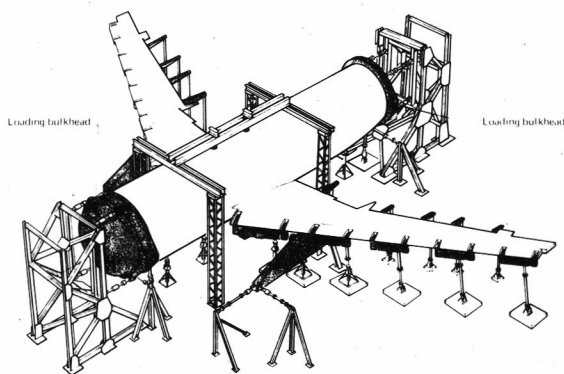


Figure 14. Fatigue Testing of the Centre Fuselage

The fatigue test covered the justification for the wing structure, the wing centre box and the fuselage section 14 from frame 33 to 39 sections 15, 16 and section 17 up to frame 69.

Section 14 from frame 26 to 33 and section 17 from frame 69 to 72 were considered as a transition structure for correct loading distribution.

#### C) Rear Fuselage Test

The rear fuselage specimen was tested in the MBB-factory at Hamburg-Finkenwerder. As can be seen from Fig.15 the rear fuselage was cantilevered aft from a pressure bulkhead. All the applied ground and flight loads were reacted at the bulkhead.

The test specimen comprised:

- the primary structure of fuselage section 17 (comprising frame 65 to 72) sections 18 and 19, including doors and windows
- the passenger floor between frames 73 and 76
- the cargo hold floor between frames 67 and 70
- the primary structure of the fin box up to rib 16

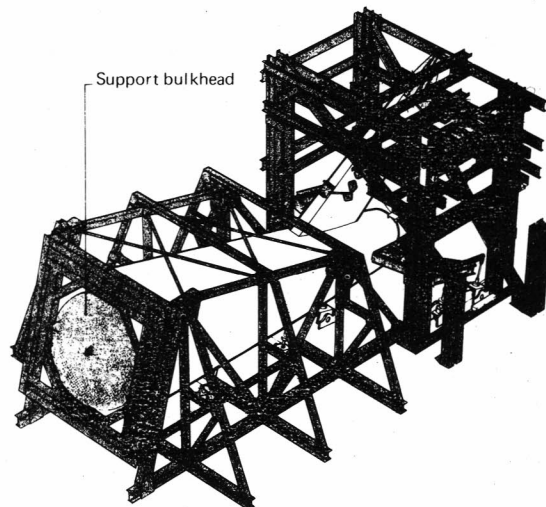


Figure 15. Fatigue Testing of the Rear Fuselage

The fatigue test covered the justification for section 17 from frame 69 upwards, section 18, 19 and the fin box up to rib 16.

The tailplane was represented by a dummy which formed a loading rig. Section 17 from frame 65 to 69 was considered as a transition structure for correct loading distribution.

#### Test Spectra

The test spectrum was based on the average utilisation of the aircraft in service. The resulting standard mission defined a flight of 65 min. flight-time and cruise flight at 29000 ft. at Mach 0.8. The average payload factor of 65% has been chosen to be larger than typical values of similar aircraft to account for the high cargo capacity of the A 300.

The standard mission includes 30 flight phases which for test purposes were reduced to 5 main



phases, resulting in equivalent damage for the fatigue critical elements, i.e.:

- taxiing and take-off
- climb
- cruise flight
- descent and stand by
- landing and taxiing

#### Taxiing

The load factor  $\Delta n_z$  spectrum for taxiing has been established from the data derived from 4 runways of varying roughnesses (Toulouse, New York, Washington and San Francisco).

#### Braking

The variation of the loads  $\Delta n_x$  when braking and towing, and  $\Delta n_y$  when turning, have been derived from statistics taken mainly from measurements made on "Caravelle" and "Concorde".

#### Landing

Descent speed measurements made on comparative aircraft in service showed a max. descent rate between 5 and 7.5 feet/sec. To be on the safe side, the maximum value of the landing impact spectrum has been raised to 9 ft/sec. The spectrum shape was defined according to the "Taylor-distribution".

#### Gusts

These were based on the RAeS Engineering Sciences Data, item 69023, considering the curves for "climb and descent" and "Aircraft with cloud warning radar".

Taking into consideration the special A 300 wing-characteristics the vertical gust frequency quoted in the above document has been increased by a dynamic response factor of 1.5 during the high speed flight phase.

Horizontal gusts were assumed to have the same frequency as vertical ones. However investigations have shown that the intensity of horizontal gusts is higher than vertical ones. This higher intensity was taken into account by allocating an intensity amplification factor of 1.15.

#### Manoeuvres

The longitudinal manoeuvre spectra for revenue flights and training flights are based on measurements performed by the Laboratorium für Betriebsfestigkeit (LBF) in Darmstadt, Germany.

For revenue flights, the mean value in the manoeuvre spectrum was assumed as 0.9 g acceleration at the C/G of the aircraft. The crew training flight spectrum mean value was fixed at 1.32 g. Ratio of crew training flights to normal flights was 1:49 defined chosen according to DLH statistics.

Recent measurements made by the LBF on the B707 have shown the importance on fatigue life of rudder manoeuvres, including engine failures during crew training flights. Therefore the same frequencies and distribution have been chosen as for longitudinal manoeuvres.

For training flights the upper boundary of the

load spectrum was assumed to be identical to the limit manoeuvre load.

#### Cabin pressure

Cabin pressure was applied once per flight to a constant differential pressure of 570 mb = 8.25 psi. The cabin pressure spectrum applied during fatigue testing was of a rectangular distribution and considered to be conservative compared to past performance of similar aircraft in service.

Since all the production aircrafts are subjected to the proof pressure  $1.33 \Delta p = 850$  mb prior to the first flight, the fatigue test airframe was also subjected to the same pressure before starting the fatigue test.

#### Engine Thrust

The A 300 is powered by two high by pass ratio engines (CF6-50 or JT9D-70) of the 51000/53000 lb category. During the tests, engine thrust was applied to the engine pylon reflecting all thrust variations of the typical mission.

#### Loading Program

The flight profile and the associated load spectra, which were the basis of the applied fatigue loads, have a major influence on the fatigue life to be demonstrated by fatigue testing.

Thus it appeared necessary to derive the test loads from so called average flight profile and load spectra with an appearance probability of 50% (following the FAA terminology, a typical flight profile, i.e. 50% of all the aircraft in service will encounter loads which are equal or lower than those defined in the fatigue load programs).

The final load spectra, defined by their max. values, cumulative frequency and the distribution shape, were established according to a method developed by the "Laboratorium für Betriebsfestigkeit".

These load spectra led to the aircraft specific "bending moment spectra" by means of dynamic calculation on the flexible aircraft.

Loads were applied in a "flight by flight" program according to the procedure developed by J. Schijve. Therefore 6 flight types A to F, relative to the different weather conditions, were established, differing in the number of load cycles and in load intensity.

Fig. 16 shows stress spectra measured in the centre fuselage test for two different flight types in the fuselage skin at frame 58, stringer 3/4.

### VI. Fatigue Failures and Crack Growth Rates in Full Scale Tests-Comparison with Calculation

Damage documentation was established on every fatigue failure in the three test cells, giving the details of the damage and informing on the progression of tests.

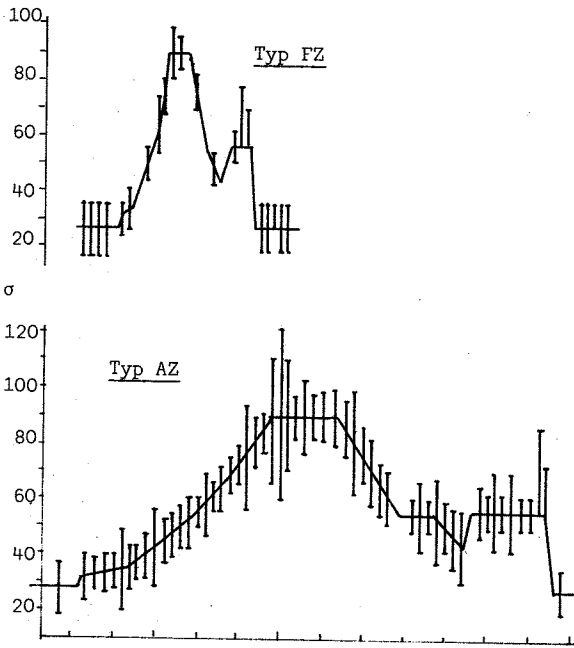


Figure 16. Skin Stresses between Frame 58 and Stringer 3-4 Measured at the Centre Fuselage Test

In addition the propagation of natural and artificial cracks was recorded and the crack propagation observed in the tests was compared with the calculated crack propagation.

On evaluation of the failure reports it showed that most of the failures occurred at identical, typical locations. In most cases these locations were identical to the type of failure occurring in other parts of aircraft.

The main causes for failure were:

- locally too high load transmission in the 1<sup>st</sup> rivet row of load introductions
- secondary bending
- too high dimensioning stresses, enforced deformation
- structural weak points such as open holes, sharp edges etc.

In the statistical compilation of fatigue cracks the crack propagation starting point was recorded and their frequency indicated in the following figures by the use of symbols.

The open symbols indicate that the cracked part was made of sheet metal whereas the closed symbols indicate that the part is a machined solid part. The individual symbols indicate:

- ○: crack starting from rivet hole
- ◊: crack starting from the immediate vicinity of the hole due to secondary bending
- □: crack starting from a radius
- ▼ ▽: crack starting from a straight edge

Figure	Nose Fuselage Test	Centre Fuselage Test	Rear Fuselage Test
18a	● 9x; ○ 45x	● 8x; ○ 18x	● 1x; ○ 5x
18b	○ 25x	○ 12x	-
20a	○ 39x ■ 1x; ▼ 1x	○ 12x; 2x	○ 13x □ 2x; ▼ 4x
21a	○ 13x; ■ 2x	○ 5x; ○ 1x	○ 1x; ■ 10x
21b	● 1x	● 5x; ■ 7x	● 2x
21c	● 3x; ▼ 2x □ 5x	○ 1x; ■ 6x	○ 1x
22a	○ 32x; ■ 6x ● 14x; ▼ 7x	○ 4x; ■ 2x ● 5x; ■ 3x	○ 6x
22b	○ 1x; ■ 4x	-	▼ 10x; □ 4x
23a	○ 2x; ▼ 1x □ 12x	○ 7x; ■ 6x ● 3x; ■ 1x	○ 12x
23b	◊ 8x; ○ 1x ● 3x; ● 9x	-	5x; □ 1x

Figure 17. Statistical Compilation of Cracks in Fig. 18 - 23

A few typical damages are discussed below:

1) Fatigue Cracks in the First Rivet Row Caused by too High Load Transmission and High Bending Stress

The following figures show the cumulative damage frequency in the service life for the above locations.

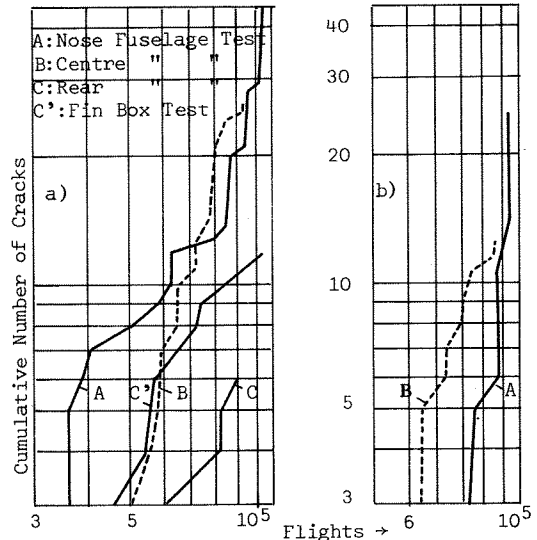


Figure 18a) Fatigue Cracks Starting at the 1st Rivet Row at Fitting (Doublers) Ends

b) Frame Cracks on Fitting Ends between Str. P40/41 (P'40/41)

The damage at the last rivet of the fitting run-out between str. 40/41 on the RH- and LH-side of the fuselage occurs relatively frequent and can be regarded as typical. Almost all frames in the centre wing box area failed in the course of tests at this runout (Fig. 19b). Figure 19a shows the same design in the case of the "Britannia" typ 100, where it failed after 6616 cycles of the full scale

test. An extension of this fitting with a tapering carried out at the same time, increased the service life in that location to 38571 flights.

This type of damage will be discussed more explicitly in the last chapter of this study.

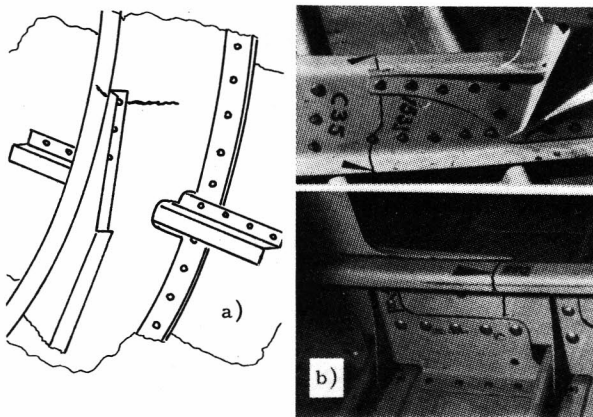


Figure 19. Fitting Runouts at Frame  
a) Britannia - 100  
b) A 300 B - Stringer 40/41

### 2) Fatigue Cracks in the Skin Panels

Figure 20 shows fatigue cracks in the fuselage and the fin box skin panels. Most of the cracks propagated very slowly, so that repair during the tests was not necessary. The skin cracks occurring relatively early in the rear part of fuselage test were initiated by local buckling of the skin areas. No further propagation of these cracks could be observed.

All skin cracks in the fin box skin started from rivet holes. More than 50 fatigue cracks, which had to be partly repaired, occurred between 50000 and 100000 test flights. This result was not satisfactory. Arrangements were made for a structure reinforcement of about 20%. Curve C'-2 shows the increase in life to be expected whereas in this case the points of curve C'-1 were calculated in agreement with their local reinforcement as to the equation:

$$N_{C'-2} = N_{C'-1} \cdot x^4$$

### 3) Failures of Frames Starting from Continuous Riveting or from Tooling Holes - Failures of Clips and Stringer Couplings

Figure 21a shows fatigue failures at the frame clips, where crack propagation starting from the riveting but also at the clip radii could be observed.

Figure 21b shows the failures in the stringer couplings. All failures of couplings in the test of the fuselage centre part occurred between frame 40 and 54, where the parts had not been shotpeened. All stringer couplings with the exception of 12 in the rear part of the fuselage (about 700 items) had been shotpeened with high intensity. The 3 coupling failures which occurred in the last mentioned fuselage section belonged to those 12 stringer couplings which had not been shotpeened.

Figure 21c shows that in contrast to the frame damages shown in Fig. 19b relatively few fatigue cracks in the frames occurred at tooling holes and continuous riveting.

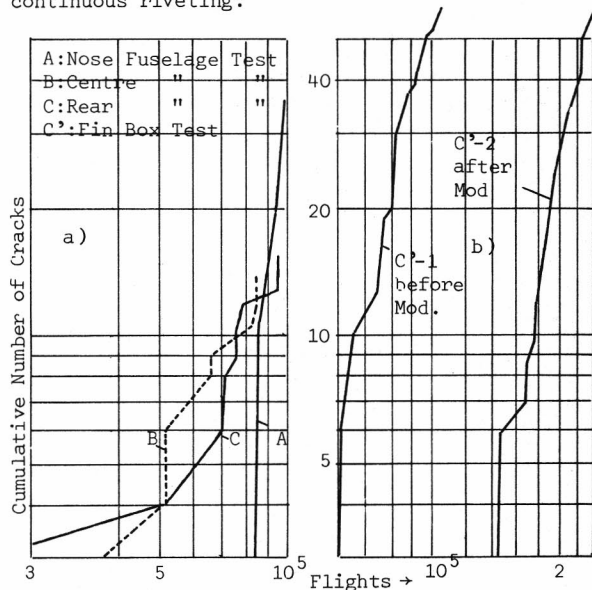


Figure 20 a) Cracks in Fuselage Skin  
b) Cracks in Fin Box Skin

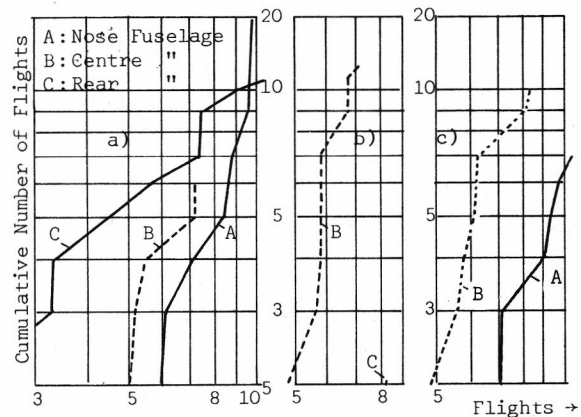


Figure 21 a) Cracks in Frame-Clips  
b) Cracks in Stringer Couplings  
c) Frame-Cracks Starting at Tooling Holes and from Continuous Riveting

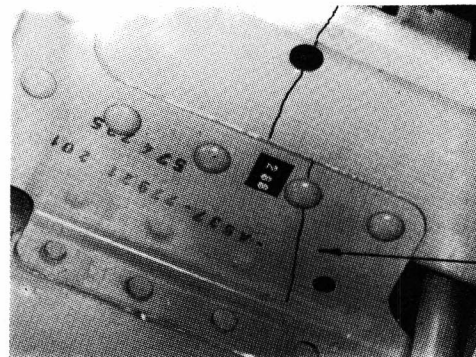


Photo for Figure 21c) Cracked Clip as Succession Damage

#### 4) Failures in Secondary Components

The following figures show typical locations in secondary components at which most of the fatigue failures occurred

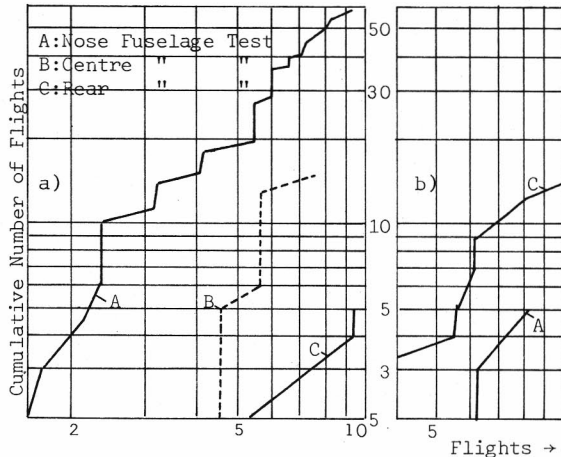


Figure 22a) Cracks in Passenger Door Frame (Covering Plates, Connecting Angles)  
b) Cracks in Frames of the Passenger Door

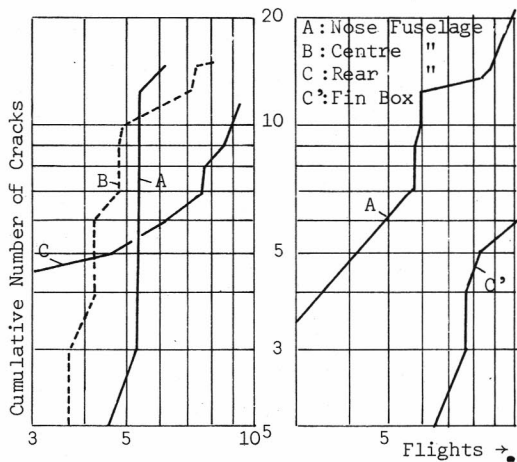


Figure 23a) Cracks in Gusset Plates, Support Angles Shear Plates and Shear Webs  
b) Cracks in Door Frame Web on Cross Connections

#### Comparison of Calculated Service Life to the Service Life Attained During Tests

At the following 3 important locations the supporting structure of the pressurized cabin was underestimated. These locations are:

- frame heads of the cargo door (frame 60 - 63)
- horizontal stabilizer cutout on fuselage (frame 87)
- fuselage longitudinal splice (frame 73 - 74 ; stringer 51)

In the case of the frame heads a load of 5 to / frame head in circumferential direction was taken as a basis for the calculated fatigue proof. The service life calculation and the fatigue tests of individual frame heads revealed more than 300000

load cycles in the case of this load.

When the forward part of the fuselage was tested at Bremen these components failed already after about 15000 cycles. Extensive stress measurements carried out at the full scale test confirmed the calculated z-load, but it showed that in addition to this load at the frame heads a deformation by force in direction of the x-axis as result of the shear deformation of the airframe occurred. This lateral displacement of a few millimeters resulted in high stresses at the blend radius from the heads to the frame which were not accounted for in the calculation.

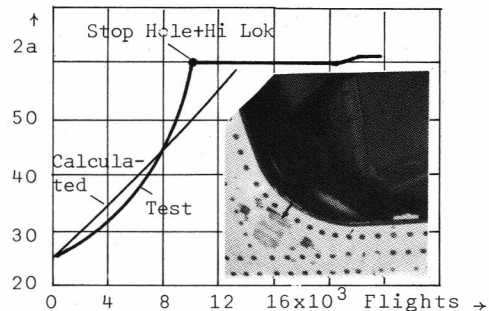
As to the horizontal stabilizer cutout an early fatigue crack formed at the runout of the corner fitting in the vicinity of frame 87 which resulted in failure of the longeron and in a skin crack of 300 mm length after 48000 simulated flights. In the fatigue calculations this location had not been considered as critical, because the critical load case had been included into the test program only lateron.

In case of the fuselage longitudinal splices a fatigue crack of 670 mm length was detected in the fuselage rear part test after 77000 flights. Extensive inspections caused by this test result and carried out at the fuselage longitudinal splices of the centre fuselage showed after 67000 test flights 4 fatigue cracks of about 4 mm length starting from the rivet holes between frame 56 - 58. Longitudinal splices of the pressurized cabin were provided with strain gauges and the stress resulting from the loads of the test flights was measured.

It showed that the additional bending stress which amounted to about 100% in the skin panel tests<sup>(1)</sup>, when internal pressure was provided amounted to more than 200% in the door areas of the overall airframe. Both in the skin tests and in the calculatory service life determinations, the locally acting maximum stress in the longitudinal splice had been underestimated.

Though all of the above mentioned locations had been fail-safe designed, they were improved by appropriate modifications so that the service life of the aircraft was essentially extended. Instructions to incorporate appropriate modifications for production and retrofit solutions into aircraft which had already been delivered could be issued in due time.

The following figures show by extract the comparison of the determination of crack propagation by way of calculation (without taking lateral contraction into consideration) and test of 35 artificial cracks in the rear fuselage test.



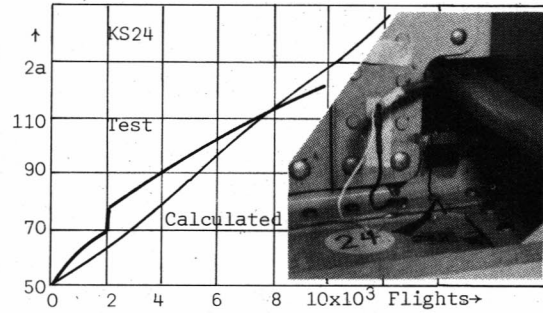
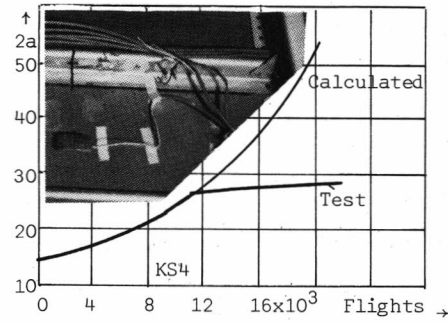
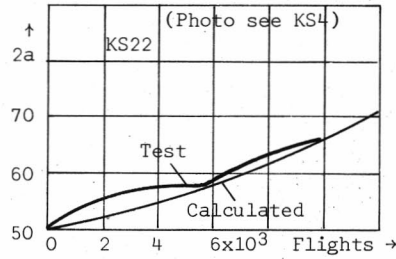
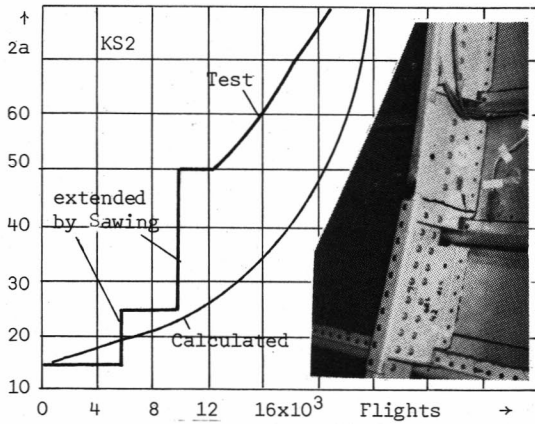
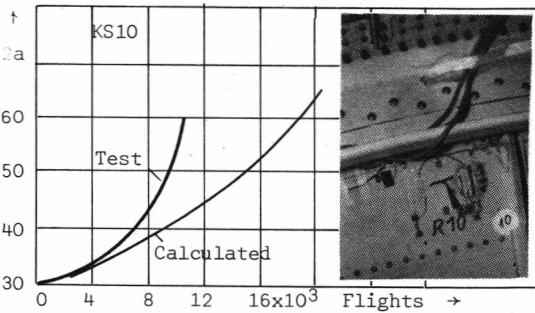
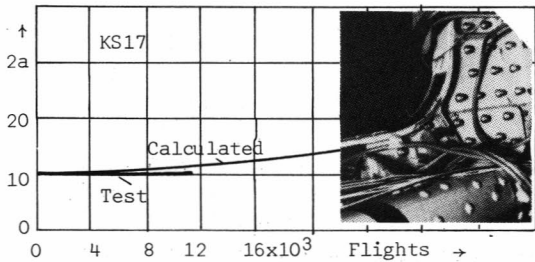


Figure 24. Propagation of Artificial Cracks in the Rear Fuselage Test



- KS1: Crack in cargo door corner
- KS2: Skin crack under separated frame
- KS4: Skin crack under separated stringer
- KS10: Skin crack in pressurized bulkhead under biaxial stress
- KS17: Corner fitting in horizontal stabilizer cutout on fuselage
- KS20: Connection fin box-fuselage
- KS22: Skin crack in fin box under separated stringer
- KS24: Skin crack in fin box under separated spar



The comparison of all crack propagation calculations and the test results showed that in the case of a biaxial stress in the field (a-both stresses positive) the stress intensity factor in the crack propagation calculation must be reduced as a function of the intensity of the 2nd stress by about 15% in order to achieve a certain degree of conformity with the test results. Even in a single-directional loaded field the stress intensity and thereby also the crack propagation rates are overestimated when the crack occurs in the immediate vicinity of a parallel installed stiffener (KS2; KS24). These transverse stiffener components apparently prevent locally the lateral contraction, so that the crack cannot open completely and thereby the stress intensity at the crack peak cannot be built up fully.

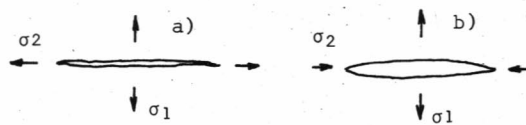
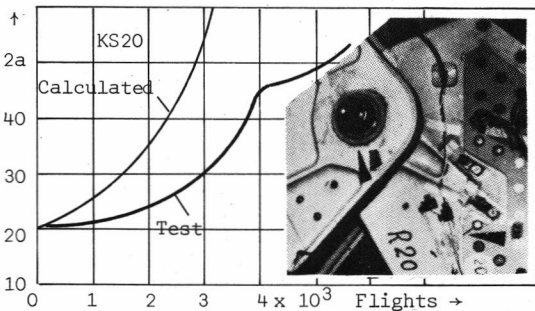


Figure 25. Biaxially Loaded Skin Cracks

On the other hand a relevant increase in stress intensity and crack propagation rates could be observed for that case when the 2nd stress direction parallel to the crack was negative and amounted to 50% of the 1st positive stress (Fig. 25b). In the latter case the crack propagation determined by test could only then be simulated by calculation if the stress intensity factor in the calculation was increased by 40%. The negligence of the compressive stress directioned parallel to the crack in connection to the tensile stress acting vertically to the crack would cause a substantial under-rating of crack propagation. If you compare the correction factors mentioned in this connection with the information of future literature, the statement is allowed, that the literature factors which are given for the consideration of biaxial stresses will be substantially smaller for both cases than the above given values(7).

### VII. Constructive Measures to Increase the Crack Free and Cracked Service Life

Service life tests of major assemblies and full scale tests confirmed anew that the load introductions not only cause a minor crack-free service life than the undisturbed structure or a continuous riveting but also that cracks occurring at the fitting runouts (last rivet row) propagate substantially faster than in a continuous riveting.

This phenomenon can be traced back to the influence of the stiffener on the stress intensity. In general a distinction is made between 3 types of crack:

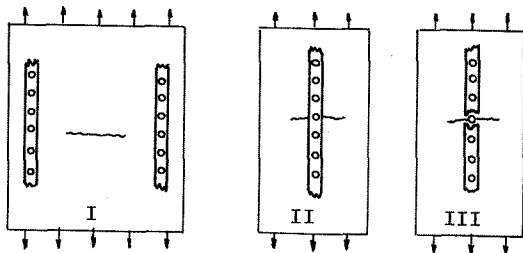


Figure 26. 3 Main Types of Skin Cracks in a Reinforced Field

Type III includes cracks occurring at a fitting runout.

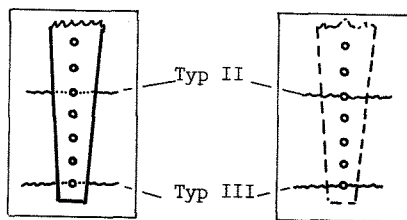


Figure 27. Skin Cracks under an Intact Fitting

If it could be achieved by appropriate constructive measures that the fatigue crack does not occur in the last rivet row of the fitting but at some preceding rivet rows, i.e. below the intact

fitting, then crack type III would have been changed into crack type II. The minimum gain due to this measure would be a doubled service life in crack-free and cracked condition.

The reasons for crack initiation in the last rivet row are the following:

- too high load transmission
- secondary bending stress
- high nominal stress (no support of the fitting section)

A well-proven measure is to taper the fitting, so that by suitable division of the loads on the rivets the centre rivet rows in the skin show the same or even a slightly higher failure probability than the last rivet row. The gain in service life by such a measure is not very high as is well known. In most of the cases the fitting itself fails.

This problem was first of all encountered in the skin panel test with windows where cracks in series occurred in the 1.6 mm skin at the clip end rivets after about 62000 test flights.

By the following comparative fatigue tests on suitably stiffened brackets with clips riveted on, constructive measures promising an increase in service life were investigated.

Test Series	Counters. related Depth	Life
a) basis version (LM-countersink rivets 4Ø)	1,4 mm	1,0
b) end rivets 4Ø mushroom head	0	2,1
c) end rivets 4Ø countersink (Ti)	1,1 "	5,4
d) " " " " (LM)	0,97 "	6,7
e) all " " " (LM)	0,97 "	9,1
f) as sub b) above, but however end riveting stresscoined as per "Douglas"	0	12,3
g) as sub d) above, but however end riveting stresscoined as sub f)	0,97	6,7
h) as sub a) above, but however end riveting ringcoined as per "Douglas"	1,4	16,0

As can be seen, the service life increase can either be achieved by quality improvement of the fatigue properties of the last rivet row (b,f,g,h) or by installation of a softer rivet (rivet head height 1.0 - 1.1 mm).

In case of the test series c, f, g, h the skin cracks partly did not occur at the end rivet row (crack type III) but at one of the centre rivet rows (crack type II). The cracked life of the specimen was extended by a factor of about 4.

Types c) and d) were the cheapest solutions and they were selected for the series production. In the course of full scale tests with the sections of the pressurized cabin, where clip riveting was performed as to c) and d), no fatigue failures occurred at these locations.



After 48000 test flights a fast propagating fatigue crack occurred in the end rivet row of the reinforcement corner fitting at the L/H horizontal stabilizer cutout; the crack occurred in the course of the full scale fatigue test of the fuselage rear part. This fitting had been installed after 10000 test flights. When the crack was detected, the longeron (cross section 120x96, 5 thick) and the reinforcement bracket (2,5 thick) were cracked. The investigation of the R/H fuselage side showed small cracks at the same location of the fitting runout. All parts were repaired and the length of the corner fitting was increased.

The Hi Lok-rivets in the old version had been installed with interference. In the modified version the fitting was provided with bore holes in the last two rivet rows, exceeding the rivet diameter by 0.4 respectively 0.8 mm. All rivet holes in the reinforcement bracket and in the longeron were press-fitted as in the old version. By this modification the following was achieved:

- in case of the last two rivets of the runout the load is transferred not via bearing pressure but only by frictional closure. By this measure load transmission and additional bending stress are reduced at this location.
- the location of fatigue failure is displaced inward for at least two rivet rows. In the case of the centre rivet rows, load transmission as well as additional bending stress are also small. This warrants a considerable increase of the crack-free service life. A possible crack at one of the centre rivets of the new type would be held together by the intact fitting located above. Crack propagation would then be considerably slower.

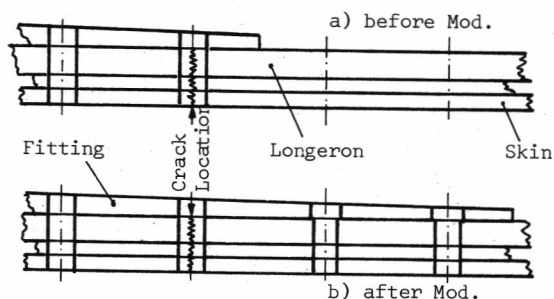


Figure 28. Modification of the Fitting Runout on Horizontal Stabilizer Cutout (Fuselage)

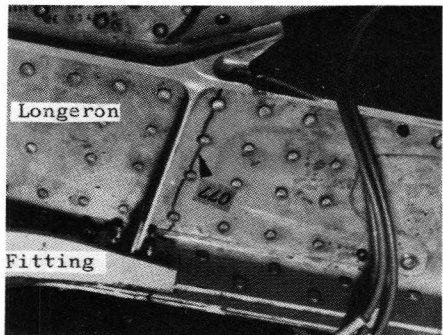


Photo for Figure 28a Skin, Bracket

The fitting, the longeron and the reinforcement bracket were provided with 38 strain gauges (partly flexa gauges). For the purpose of comparison stress measurements for the different flight phases were performed with a short fitting at first and then with the new type. It showed that the nominal stress at the location A is reduced by about 30% and the additional bending stress at the new type of runout becomes smaller. In the further course of the full scale test up to 106000 test flights no failure could be observed at this location.

Comparative tests carried out for the run-out of the fuselage attach fittings at the wing underside of the F104, showed on incorporation of the above mentioned design modifications improvements in service life exceeding a factor of 10.

The same design principle was accomplished in the Airbus design at the vertical stabilizer skin runout, at the fuselage attach fittings, at the corners of the emergency exit at the rivetings of the steel reinforcements brackets.

Further weak points are the frame heads of the cargo doors which failed in the course of centre parts of fuselage full scale test after about 48000 test flights and after 15000 test flights in the nose fuselage test. In spite of the fail-safe design of these door hinges (7-point suspension) the service life had to be increased.

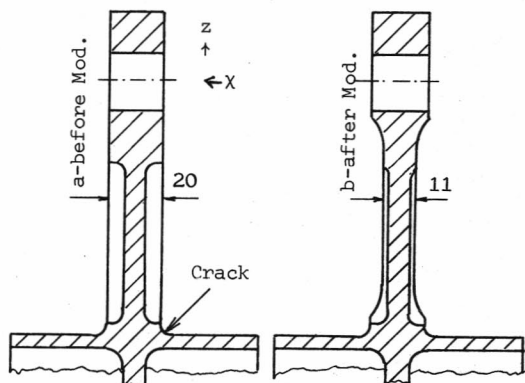


Figure 29. Modification of the Frame Heads on Cargo Door (Frame 60-63)

Shotpeening of the failure-endangered blend radii brought about no life improvement. The application of strain gauges at these blend radii showed that the  $E \cdot \epsilon$  - values at this location by far exceeded the yield strength of the material. It is understandable that the effect of compressive stress, which is built up by shotpeening at the surface of the notch is lost at this high tensile strains.

After the cause of failure had been determined by extensive deformation and stress measurements - deformation by force of the frame heads in direction of the x-axis caused by shear stress in the fuselage skin - the solution was simple. The frame heads were tapered in the direction of the x-axis from 20 to 11 mm. Due to the fact that the web became more resilient, the stresses in the blend radius were reduced by 1/3 in the case of the same load case combined with internal pressure. Comparative fatigue tests, carried out at the individual frame head resulted in a service life increase



by a factor of about 5. The already installed old type frame heads in already delivered aircraft and at the test cells were laterally milled and shot-peened as shown on Fig. 29. After this modification had been carried out, no fatigue failures occurred at these locations in the course of the full scale tests.

Extensive strain measurements in the course of centre part and rear part of fuselage full scale test showed that the longitudinal splices in the door areas have a considerably higher additional bending stress than expected and that the service life requirements were not completely met at these locations. For the reduction of the additional bending stress and thereby increase of service life, a repair solution should be found which is also applicable in the case of already delivered aircraft without taking much modification trouble.

Comparative life tests of appropriately shaped rivet specimens were carried out whereby the high additional stress, measured at some locations in the pressurized cabin was maintained in the case of the small specimens by reduction of the rivet pitch.

The following lists the investigated versions:

Version	related Life
1. basic type	1.0
2. basic type with DPS ringcoining	1.17
3. basic type with supporting angle	1.84
4. basic type with pre-connection 1.2 mm thick	1.52
5. as under 4. above, pre-connection 0.8 mm	1.57
6. with T-type stringer	>1.84

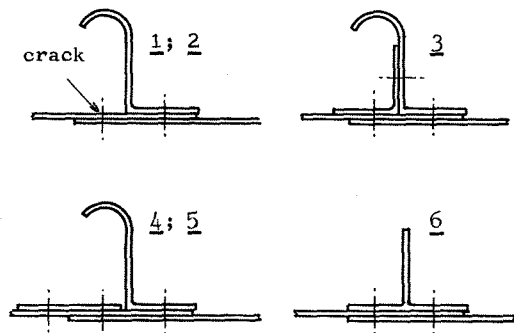


Figure 30. Measures to Improve the Fatigue Strength of the Longitudinal Skin Splice (Frame 73; Str.51) of the Pressurized Cabin

The supporting angle version was selected as retrofit solution for the already constructed aircraft and for the test cells. Stress measurements carried out for the purpose of comparison prior to and after the retrofit of the test cells showed a reduction of the maximum stress (tension + bending) in the case of an internal pressure load case by 15%. Thereby the aim of service life was achieved.

For reasons of cost the solution using the T-type stringer (version 6) was chosen for new production.

### Symbols

- a: Half crack length (mm)
- $B_1$  ( $B_2$ ): Thickness of skin (stringer) (mm)
- $C_1$  (C): Factor due to cabin pressure (geometrical factor) to effect the stress intensity
- $C_V$ : Stress ratio at the crack tip
- d: Rivet diameter (mm)
- da/dn: Crack propagation rate under cyclic load
- EN; EH;  $E_{str}$ : Modulus for rivet, skin and stringer material ( $N/mm^2$ )
- FH: Flight hours
- FF ( $F_{str}$ ): Cross section of frame (stringer) ( $mm^2$ )
- $I_I$ : Inspection Interval (hours)
- K ( $\Delta K$ ): Stress intensity (amplitude) ( $Nmm^{-1,5}$ )
- $K_C$ : Fracture toughness ( $Nmm^{-1,5}$ )
- $L_S$ : Stringer load factor
- M; n: "Forman" constants
- N: River load (N)
- PA: Probability of failure
- $\Delta p$ : Cabin pressure ( $N/mm^2$ )
- R: Stress ratio ( $\sigma_{min}/\sigma_{max}$ )
- $\delta$ : Rivet deflection (mm)
- $\tau$ : Shear stress ( $N/mm^2$ )
- $\sigma_B$ : Nominal stress (bending stress) ( $N/mm^2$ )
- $\sigma_C$ : Residual strength ( $N/mm^2$ )

### References

- (1) Winkler, "A 300B Detailversuche CV" ES 113/69 -Ausgabe 12.73 - Deutsche Airbus GmbH München
- (2) Königsmann, H., "Programm zur Berechnung von Versteifungsfaktoren bei versteiften Schalen" Unveröffentlichter MBB UH-Bericht
- (3) Swift, T.; Wang, D., "Damage Tolerant Design Analysis Methods and Test Verification of Fuselage Structure" AFFDL-TR-70 (1970)
- (4) Gökgöl, O., "A 300B-EF3/SM3 - Vorschlag zur Verstärkung der Radialversteifungen" MBB UH-A 300B Bericht Nr. 19//A002.74937/2
- (5) Soreadhiningrat, B., "Programm zur Berechnung des Ribwachstums und der Restfestigkeit" MBB UH -Bericht Nr. 00//A007.74731
- (6) Pusponogoro, H.; Hannak, R., "Programm zur Berechnung des Ribfortschrittes in glatten und versteiften Feldern unter Berücksichtigung von Retardation" EDV-Programm (RISSFO-HABIBIE)
- (7) Gökgöl, O., "Lebensdauervorhersage für Kampf-flugzeuge - Ribwachstum und Restfestigkeit" ZTL 1976 - MBB UH Bericht Nr. UH-28-76
- (8) Koshorst, "Airbus A 300 - Full Scale Fatigue Test" AI/TE 3-769/77; Issue: April 78
- (9) Willert, U., "Ermüdungsversuch am Hautfeld mit Fenstern" A 300 B - Versuchsbericht Ev-050 (1.08.2) Deutsche Airbus GmbH München
- (10) Schütz, D.; Gökgöl, O., "Optimierung einer verschraubten Fügung zwischen Flügelunterdecke und Anschlußbeslag eines Militärflugzeuges" LBF Bericht Nr. TR-95 (1971)